Research Paper

Study of the role of leukocyte telomere length-related lncRNA NBR2 in Alzheimer's disease

Wenjie Li[1,*], Haoyan Chen[2,*], Xiaofan Yuan[3,*], Qi Yao[1], Mingjiong Zhang[2]

[1]Department of Geriatrics, The First Affiliated Hospital of Ningbo University, Ningbo 315000, China
[2]Department of Geriatrics, Jiangsu Key Laboratory of Geriatrics, The First Affiliated Hospital of Nanjing Medical University, Nanjing 210000, China
[3]Department of Radiology of the Second Affiliated Hospital of Nanjing Medical University, Nanjing 210011, China
*Joint first author

Correspondence to: Mingjiong Zhang; **email:** major2021@njmu.edu.cn
Keywords: Alzheimer's syndrome, leukocyte telomere length, mendelian randomization analysis, lncRNA NBR2, GJA1
Received: March 16, 2024 **Accepted:** July 17, 2024 **Published:** September 16, 2024

ABSTRACT

Alzheimer's Syndrome (AD) is a neurodegenerative disease that is prevalent in middle-aged and elderly people. As the disease progresses, patients gradually lose the ability to take care of themselves, which brings a heavy burden to the family. There is a link between leukocyte telomere length (LTL) and cognitive ability. To search for possible pathogenic mechanisms and potential therapeutic agents, we demonstrated a causal link between LTL and AD using Mendelian randomization analysis (MR). The expression of the target gene NBR2 and the downstream mRNA GJA1 and GJA1-related genes, pathway enrichment, and association with immune cells were further explored. Using the gene cluster-drug target interaction network, we obtained potential therapeutic drugs. Our study provides evidence for a causal link between AD and LTL, suggesting medicines that may treat and alleviate AD symptoms.

INTRODUCTION

Alzheimer's syndrome (AD) is a slow-onset and progressive brain disease. Over time, the disease progresses to severe memory problems, eventually causing patients to lose the ability to perform daily tasks [1]. AD is also one of the most common age-related neurodegenerative diseases, affecting approximately 6.5 million people aged 65 and older in the U.S. [2]. AD is, therefore, a significant challenge for global healthcare. However, the mechanisms underlying the relationship between AD and aging are unclear.

Telomeres are known as the "mitotic clock" of cell life, and their length reflects the replication history and potential of cells [3]. As we age and the number of cell divisions increases, some of the genes that make up telomeres fail to replicate fully due to multiple cell divisions, and the cell terminates its function and no longer divides [4]. Thus, severely shortened telomeres indicate cellular aging [5]. Leukocyte telomere length (LTL) is a widely used biomarker, and in general, leukocyte telomere length reflects the state of senescence of the body's immune cell-associated circulating cells [6]. It is unclear whether LTL is a risk factor for AD development.

Competitive endogenous RNA (ceRNA) networks, in which long non-coding RNAs (lncRNAs) function as endogenous ceRNAs to sequester microRNAs (miRNAs) and thereby enhance the expression of messenger RNAs (mRNAs), have been increasingly recognized for their significant contributions to the pathogenesis of Alzheimer's disease (AD) and

immune-inflammatory responses [7–9]. Among them, mir-19, a downstream miRNA of the LTL-associated lncRNA NBR2 [10], is mainly enriched in neural progenitor cells (NPCs) in hippocampal tissues, and its expression is down-regulated during neuronal development, particularly affecting neuronal cell migration [11]. mir-19-3p, the mature body of mir-19 [12], has been shown to alleviate amyloid β-induced nerve injury and thereby slow down the developmental process of AD [13].

Using two-sample Mendelian analyses, our study first explored the causal link between LTL and AD. We obtained the downstream miRNAs by intersecting the high lncRNA expression in various brain tissues and using TargetScan, followed by protein and gene level screening of NBR2-related genes to get GJA1. We further explored the function of GJA1 and its related genes. Finally, a novel drug-target interaction network framework was used to screen potential drugs to delay AD progression.

MATERIALS AND METHODS

Mendelian randomization analysis

LTL-related GWAS data were obtained from the UK Biobank, with 446,367 participants undergoing LTL measurements.

Data on genetic variants associated with AD were obtained from the GWAS database, ID number GCST90012877. $p < 1e\text{-}8$ was used as the genome-wide threshold. After screening with continuous instability and weak variable removal tools, 59 enetic instrumental variables (IVs) were finally obtained. We determined positive results and causal associations by the inverse variance weighted algorithm. The results of the MR-Egger algorithm were used as a test to assess heterogeneity. The MR egger_intercept algorithm was used to detect the data's diversity and evaluate the result's robustness. The "RCiros" package was used to visualize the chromosomal location of SNPs associated with IVs. The summary-data-based Mendelian randomization (SMR) was used to screen the eQTL corresponding to IVs and obtain the related genes [14] (https://cnsgenomics.com/software/smr/). The data on the expression of IVs-related genes in various brain tissues were obtained from the GTEx eQTL summarized data (https://www.gtexportal.org/home/eqtlDashboardPage).

Application of interaction networks

The core gene NBR2 was obtained by taking the intersection of IVs-related genes from various brain tissues. lncRNA NBR2 expression in brain tissue was obtained from http://www.alzdata.org/. Downstream miRNAs and their maturation bodies were predicted using the LncRNA2Target V3.0 database (http://bio-computing.hrbmu.edu.cn/lncrna2target/). Corresponding mRNAs were expected from the TargetScan database (https://www.targetscan.org/vert_80/). The mRNAs with |Total context++ score|>0.6 were selected for subsequent analysis. Finally, NETWORK was used for the presentation.

Functional and immunological enrichment of GJA1 and related genes

GSEA enrichment analysis of GJAI, KEGG pathway, and immune-related function was performed by "clusterProfiler." Temporal Cortex data samples were divided into a high-expression group and a low-expression group according to the target gene GJA1. The CIBERSORT algorithm demonstrated the expression group and the ratio of immune genes between different groups. The correlation between lymphocyte subpopulations and GJA1 was compared between the differences between the two groups. The GJA1-related gene clusters were screened by Spearman analysis with $-0.6 < cor < 0.8$ and $p < 0.001$. Subsequently, we visualized the GO, KEGG, immune cell correlation, and chromosomal location distribution of GJA1-related genes.

Screening of potential therapeutic drugs

Based on the Human Gene Interaction Network, we calculated the known drug's relevant target of action, its own drug's appropriate target of action, and an AD-related gene called proximity, which was converted into a z-score. P-values corresponding to the significance of each drug were computed by randomly perturbing the global network 1000 times. Based on the topological nature of the network, we performed subnetwork module mining to cluster drug targets and disease genes in each module.

Statistical analysis

We conducted a two-sample MR analysis using R software with the TwoSample MR and MR-PRESSO packages to explore the causal relationship between LTL and AD. The major method was random-effects inverse variance weighted (IVW), supplemented by MR Egger, weighted median, simple mode, and weighted mode. Heterogeneity was assessed using Cochran's Q statistic (IVW) and Rucker's Q statistic (MR Egger), with $p > 0.05$ indicating no heterogeneity. Horizontal pleiotropy was evaluated using the MR Egger intercept test and MR-PRESSO, with $p > 0.05$ indicating no

pleiotropy. MR-PRESSO also identified outliers. A "leave-one-out" analysis examined the influence of individual SNPs on the causal relationship. The MR-PRESSO global test assessed horizontal pleiotropy ($p > 0.05$), and the distortion test identified outliers, which were excluded before reassessing causal estimates. The Cross-platform normalized expression level of different genes in Entorhinal Cortex, Hippocampus, Temporal Cortex, and Frontal Cortex was assessed statistically by Student's T-test. Meanwhile, correlation between the target gene expressions was studied by using Pearson's correlation. GO and KEGG analysis were performed to calculate enrichment p-values using hypergeometric distribution tests. P-values were set at 0.05 for statistically significant differences. Data analysis was done using R Foundation version 4.2.0.

RESULTS

Leukocyte telomere length and Alzheimer's syndrome

GWAS data on leukocyte telomere length (LTL) associated with AD were obtained from open databases. The 59 SNPs strongly associated with AD after removing confounders and filtered by linkage disequilibrium and removing weak variables tools were treated as IVs (Figure 1A and Supplementary Table 1). Leave-one-out-analysis did not reveal abnormal SNP driving the association of IVs (Figure 1B). The scatter plots of the five MR analyses are shown in Figure 1C and Supplementary Table 2. The results of one of the IVW algorithms showed that LTL showed a negative correlation with AD. Heterogeneity was assessed by IVW and MR-Egger test, and p-value > 0.05 indicated no heterogeneity in the study (Figure 1D and Supplementary Table 3). Figure 1E demonstrates the location of IVs on chromosomes. As described in our previous analyses, we created a Sankey map of associated genes for IVs versus expression in various brain tissues to predict the expression of the genes related to IVs in brain tissues (Figure 1F and Supplementary Table 4).

Analysis of genes corresponding to IVs

For brain amygdala, brain anterior cingulate cortex BA24, brain caudate basal ganglia, brain cerebellum, brain cortex, brain frontal cortex BA9, brain hypothalamus, brain hippocampus, and brain nucleus accumbens basal ganglia-related genes were taken to intersect, and the core gene NBR2 was finally obtained (Figure 2A). We used the information in the AIZ database to visualize the expression of NBR2 in primary brain tissues (Figure 2B). NBR2 was used as a lncRNA, and we used miRNA-lncRNA interactions analysis to obtain the possible downstream miRNAs, mir-19A. mir-19A has the maturation bodies of mir-19-3p and mir-19-5p. Subsequent analysis was carried out using miRNA target prediction (Supplementary Tables 5, 6). The miRNA target prediction software TargetScan was utilized to analyze the miRNA-mRNA network (Figure 2C). To ensure that the gene expression levels were consistent with the protein expression levels, we screened 469 genes related to highly expressed proteins based on the results of the data from Johnson ECB et al. (Supplementary Table 7). There were 106 NBR2-related gene sets (Supplementary Table 8). Taking the intersection of protein data with gene data yielded NRXN1, ITGB8, GUCY1A2, GJA1, and DTNA (Figure 2D).

Differences in gene expression levels in primary brain tissues

We used the AIZ database information to visualize the ITGB8 (Figure 3A), GJA1 (Figure 3B), DTNA (Figure 3C), NRXN1 (Figure 3D), and GUCY1A2 (Figure 3E) in Entorhinal Cortex, Hippocampus, Temporal Cortex, and Frontal Cortex Expression. Excluding NRXN1 and GUCY1A2, which had inconsistent gene and protein expression, we found that ITGB8, GJA1, and DTNA had the most significant expression differences in the Temporal Cortex. Among them, GJA1, with Log2FC = 1.21, was the most important and was selected as our subsequent target gene.

Functional exploration of GJA1 at the single gene level

To verify the expression of GJA1 in the brain tissues of young and old populations, we can get that GJA1 is more expressed in the brain tissues of geriatric populations using immunohistochemistry data from the HPA database (Figure 4A). Using the immunofluorescence results of mouse brain tissue, we can see that GJA1 is mainly enriched in the cortical part of the brain (Figure 4B). Single gene GO analysis (Figure 4C), KEGG analysis (Figure 4D), and Immune-related function analysis (Figure 4E) were performed for GJA1. The Temporal Cortex data samples were divided into high and low-expression groups according to the expression of the target gene GJA1, and the percentage of immune genes in the two groups was compared using the CIBERSORT algorithm (Figure 4F). Further comparing the two groups' lymphocyte subpopulations, we can get T cell CD4 memory resting accounted for more in the high-expression group, and T cell follicular helper accounted for more in the low-expression group (Figure 4G). Among them, T cell CD4 memory resting was positively correlated with the expression of GJA1 ($R=0.29$, $p=0.0052$), and T cell follicular helper was negatively correlated with the expression of GJA1 ($R=0.3$, $p=0.004$).

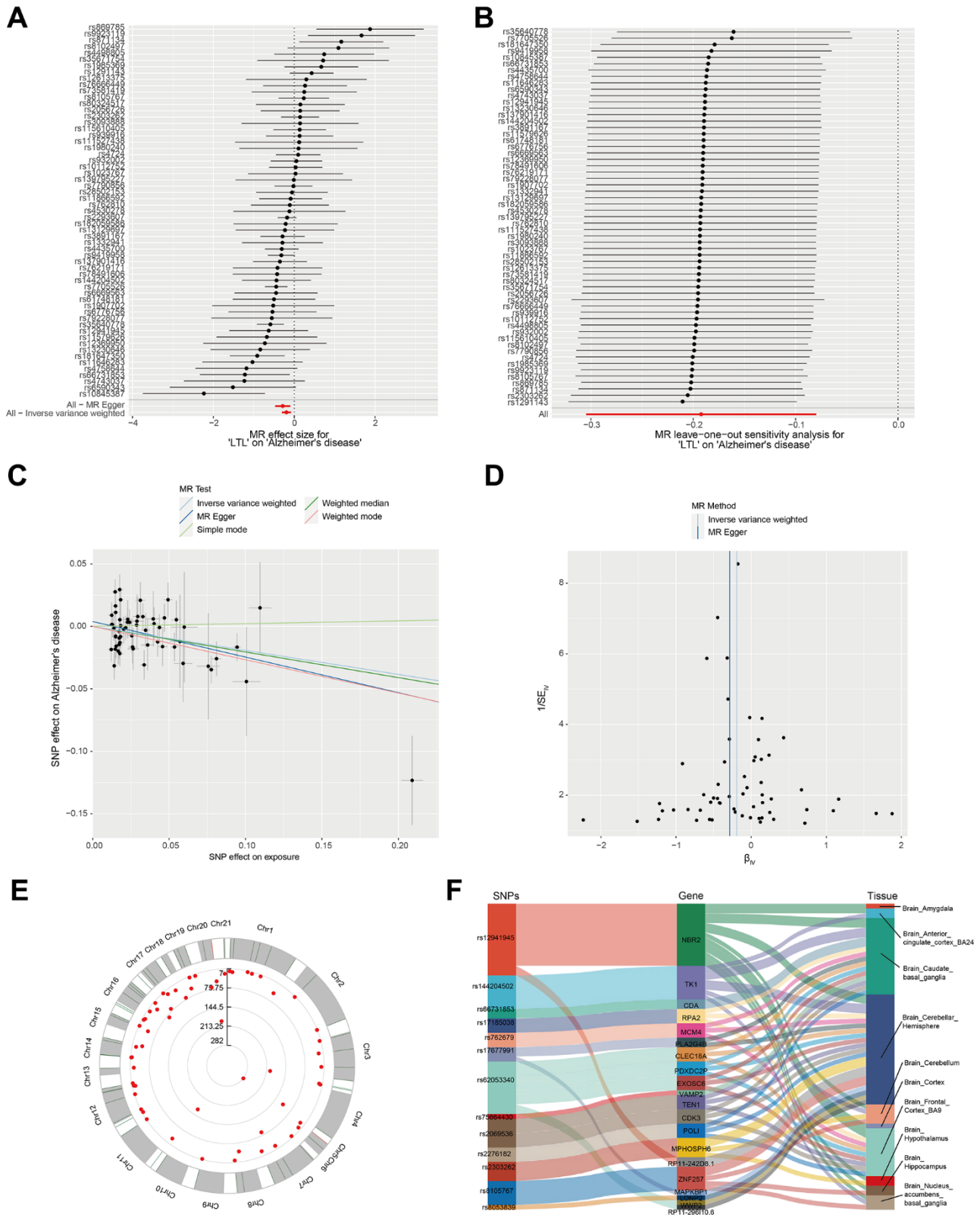

Figure 1. Verification that leukocyte telomere length is correlated with Alzheimer's syndrome using Mendelian randomization. (**A**) MR analysis for LTL on AD. (**B**) Sensitivity verification using leave-one-out analysis. (**C**) Scatterplot representing the causal link between LTL and AD. The horizontal axis reflects the genetic effect of each SNP on LTL. The vertical axis reflects the genetic impact of each SNP on the risk of developing AD. (**D**) Heterogeneity was assessed by IVW and MR-Egger tests. (**E**) Distribution of IVs associated with the location of SNPs on chromosomes. (**F**) Sankey diagram of SNP → gene ← tissue type.

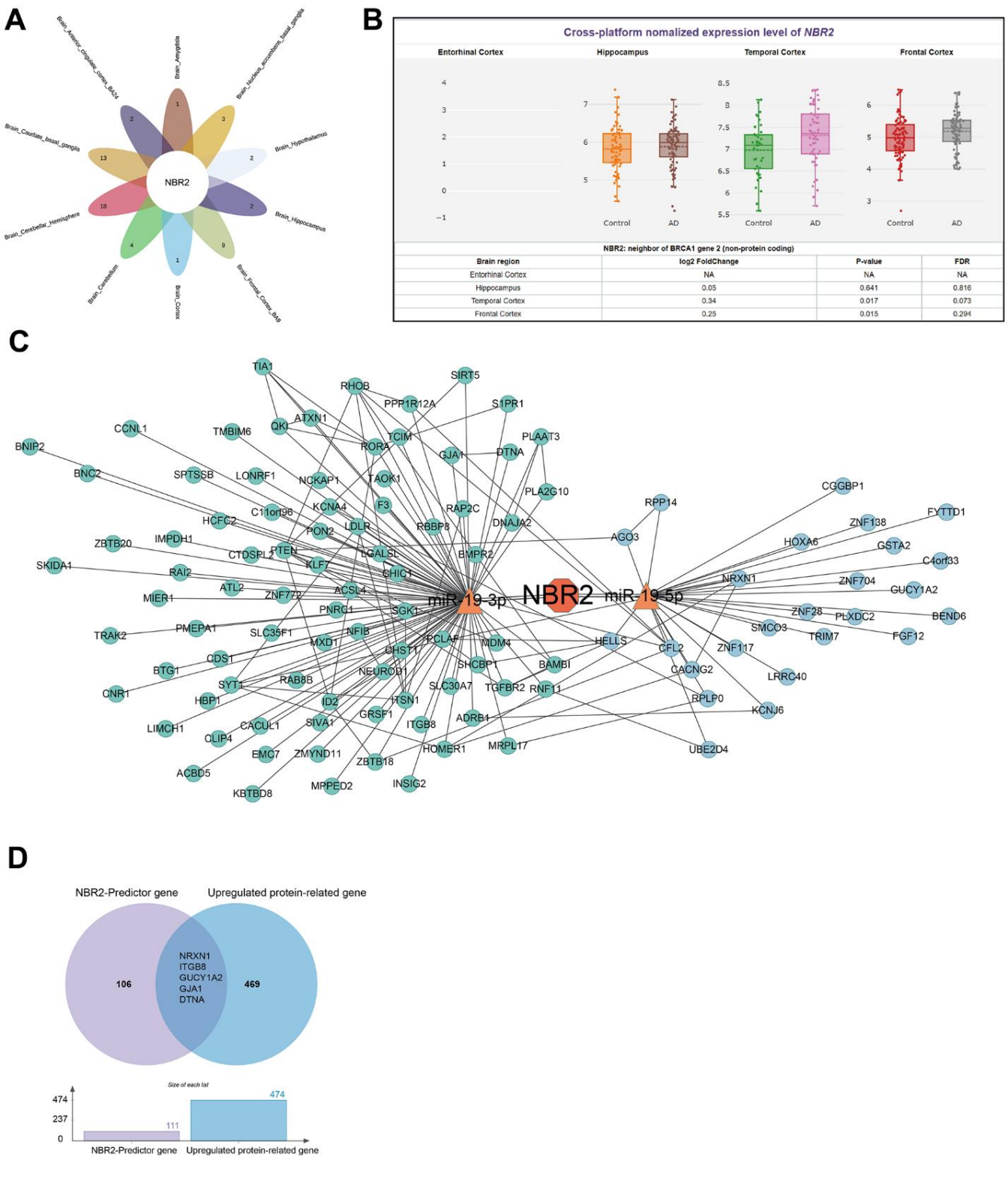

Figure 2. Analysis of genes corresponding to IVs-associated SNPs. (**A**) Venn diagram demonstrating that NBR2 is a core gene in various parts of the brain tissue. (**B**) Violin diagram demonstrating the expression of NBR2 in the significant components of the brain. (**C**) NETWORK diagram demonstrating miRNAs and mRNAs downstream of NBR2. (**D**) The Venn diagram demonstrates the high expression of 5 genes at both the protein and gene levels.

Potential expanded functions of the GJA1

We further explored the scalable functions of GJA1 in-depth and screened the genes closely related to GJA1 using Spearman analysis with p<0.001, -0.6<cor<0.8 (Figure 5A). Finally, 18 related genes were obtained, which were GABRG3, RASGRF1, IDH3G, BEND5, NOTCH2, ATP1A2, CSRP1, GRAMD1C, PLSCR4, GRAMD3, HSPB3, ICA1, GFRA2, SLC39A12, GOT1, ADD3, PAX6, CCNA1. Figure 5B shows the chromosomal location distribution of GJA1-related genes. GO analysis suggested that GJA1-related genes were mainly enriched on the plasma membrane (Figure 5C and Supplementary Table 9), and KEGG analysis suggested that they were mainly enriched on the Ras signaling pathway (Figure 5D and Supplementary Table 10). The linkage of GJA1-related genes with immune cells is shown in Figure 5E.

GJA1-related gene set prediction of potentially targeted AD drugs

Based on the assumption that drugs are effective by targeting proteins within or near the corresponding disease module, we introduced an unsupervised and unbiased network framework to analyze the relationship between drugs and diseases. By linking the interactions network of drug targets with GJA1-related genes, we finally predicted that Adapalene, Rubidium Rb-82, Ammonia, Hexachlorophene, Vorinostat, Valine, Potassium gluconate, Ouabain Cyclothiazide, Chlorthalidone, Mangafodipir, Cefotaxime, Cefalotin, Tranexamic acid, Cefmetazole, and Cefpiramide are potential target drugs (Figure 6A). Based on the topological nature of the network, we then performed subnetwork module mining to cluster the drug targets and disease genes in each module (Figure 6B).

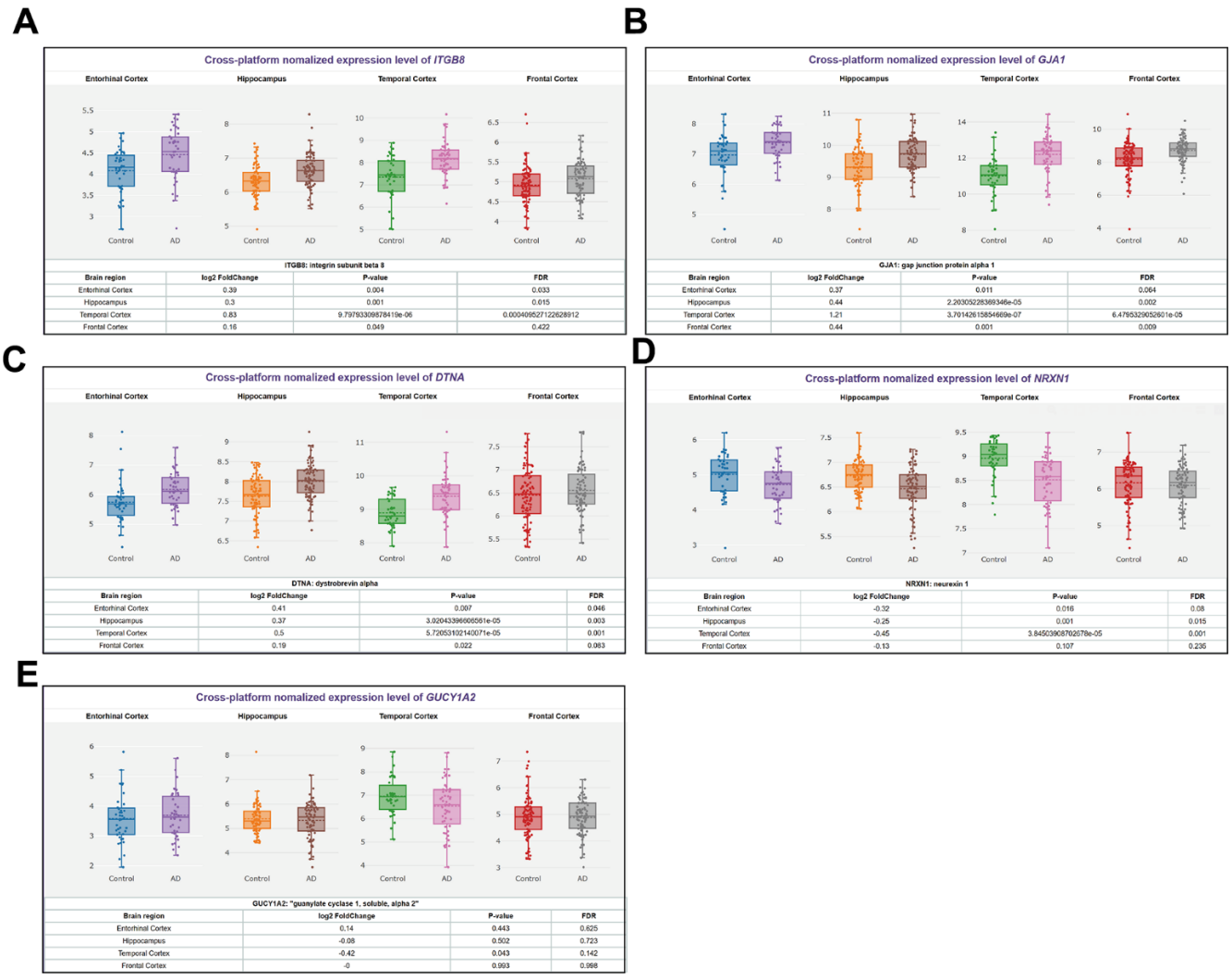

Figure 3. Differences in expression levels of 5 predicted mRNAs in primary brain tissues of AD patients. (**A**) ITGB8, (**B**) GJA1, (**C**) DTNA, (**D**) NRXN1, and (**E**) GUCY1A2 expression in Entorhinal Cortex, Hippocampus, Temporal Cortex, Frontal Cortex.

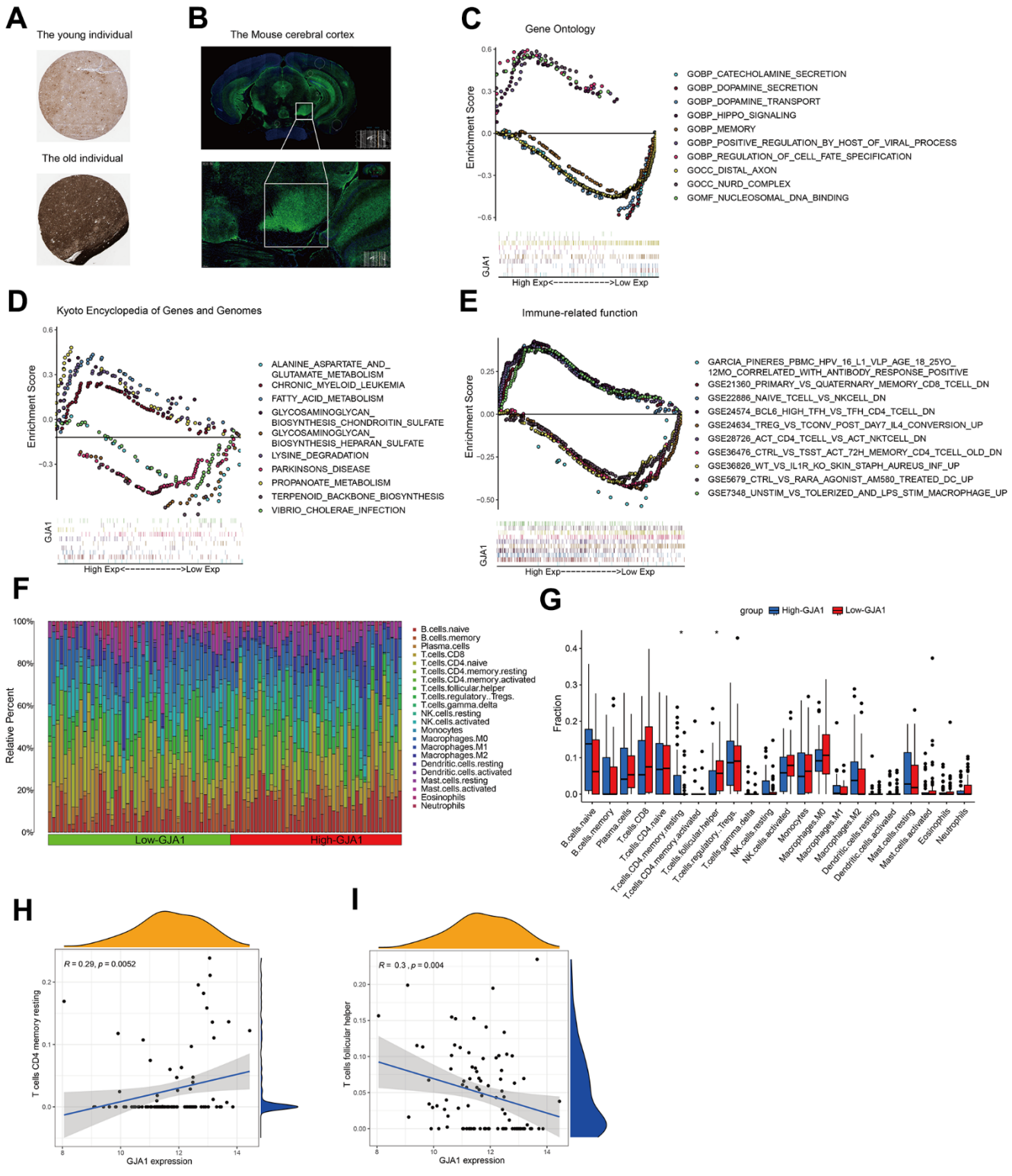

Figure 4. Functional exploration of GJA1 at the single-gene level. (**A**) Immunohistochemistry results demonstrating the expression of GJA1 in older populations. (**B**) Immunofluorescence demonstrating the enrichment of mouse brain tissue for GJA1 in the cortex. (**C**) GO analysis of GJA1. (**D**) KEGG analysis of GJA1. (**E**) Immune-related function analysis of GJA1. (**F**) Percentage of immune cells in the immune cell ratio between groups with high and low expression of GJA1 in Temporal Cortex. (**G**) Lymphocyte subpopulation occupancy in the two groups. (**H**, **I**) Correlation between lymphocyte subpopulation and GJA1 in the two groups.

DISCUSSION

LTL is commonly associated with aging, with data from a UK biobank of over 450,000 individuals suggesting a link between LTL and human health status [15]. Several studies have suggested a link between LTL and age-related cognitive decline in older adults. In a survey by Daniela et al., LTL shortening in AD patients appeared

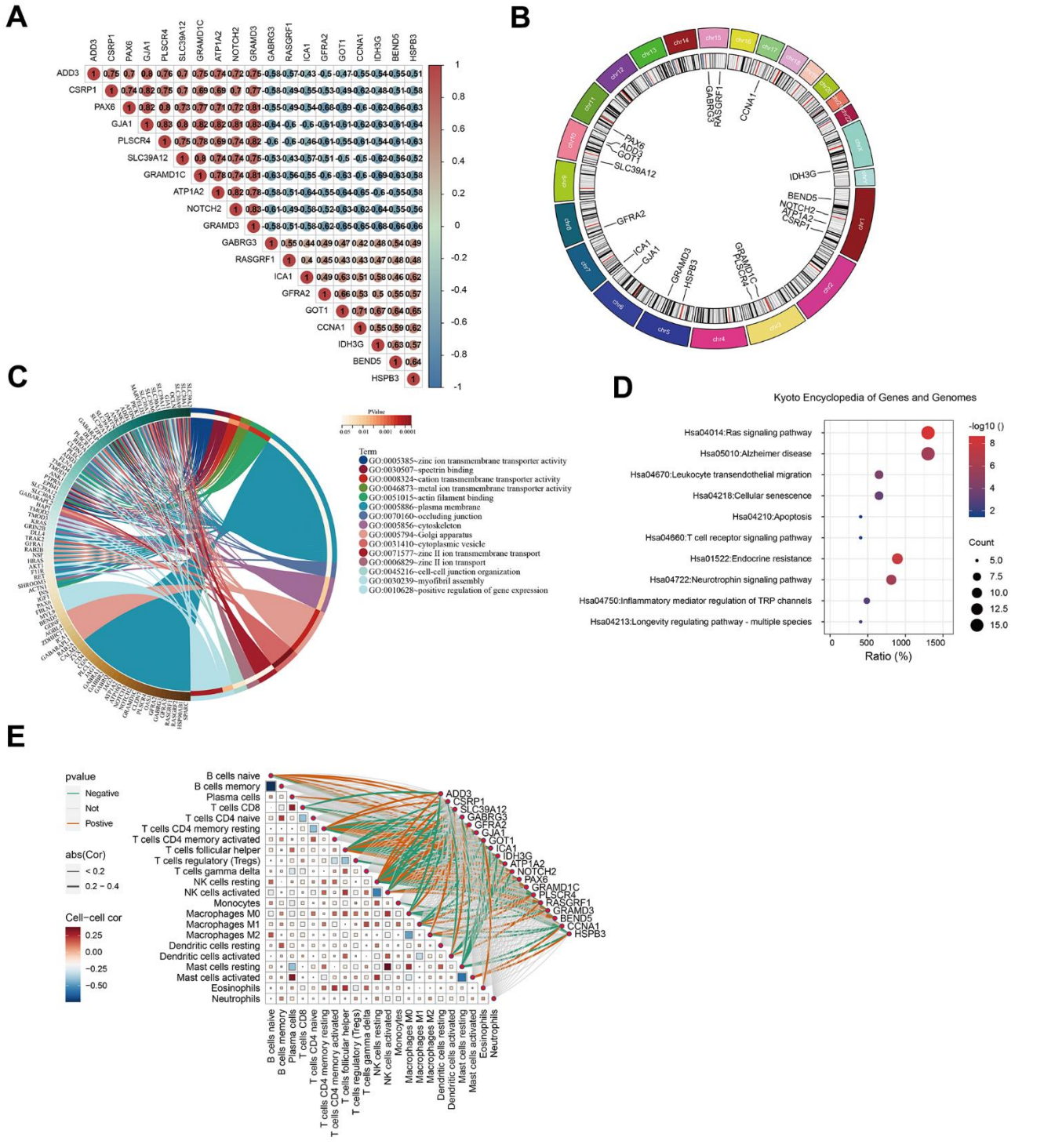

Figure 5. Analysis of GJA1-related genes. (**A**) Heatmap showing GJA1-related genes. (**B**) Chromosomal location distribution map of genes related to GJA1. (**C**) Circle map of GO analysis of the genes related to GJA1. (**D**) Circle map of KEGG analysis of the genes related to GJA1. (**E**) Correlation of the genes related to GJA1 with the immune cells.

to arise from progressive telomere erosion, which may be associated with cognitive decline in the transition from aMCI to AD [16]. From another perspective, reduced LTL indicates active cell proliferation and may reflect the immune system's involvement in AD pathogenesis [17]. However, in some studies, this association was relatively minor or absent [18]. Based on this, we hypothesized that in peripheral leukocytes, telomere length is associated with an increased risk of age-related phenotypes. We then used Mendelian randomization analysis to explore the causal link between AD and LTL, filling in the gap at the SNP level.

80% of the human genome is non-coding RNAs involved in various biological functions [19]. There is

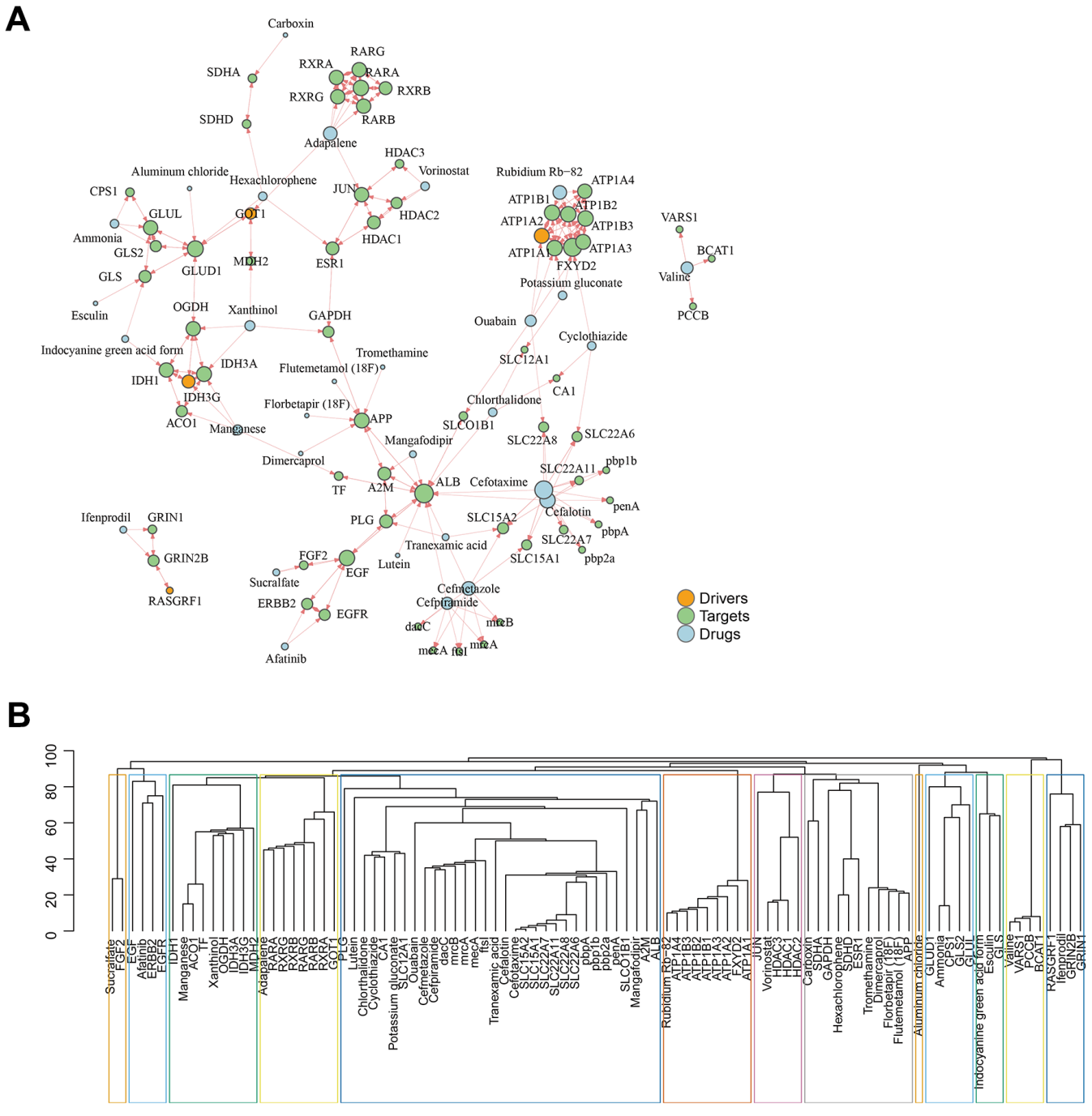

Figure 6. GJA1-related gene set predicts subsequent AD-targeted drugs. (**A**) Network diagram showing predicted drugs and targets. (**B**) Drug targets and disease genes are clustered in a module.

evidence that miRNAs and lncRNAs are simultaneously engaged in AD ontogeny and development, including the formation and development of β-amyloid (Aβ) plaques, neuro progenitor fiber tangles, synapse loss, and neuronal death [20]. And they have specific temporal and spatial expression patterns. This suggests that LTL, our "aging clock," is associated with lncRNAs, so we used the bioinformatics data from the AIZ database to select NBR2, a lncRNA with high expression of IVs-related genes in brain tissues, as the main entry point for our study. It interacts with AMPK and enhances AMPK activation under energy stress, thereby mediating cellular energy metabolism [21]. Currently, it is mainly used as a biomarker in hepatocellular carcinoma, colorectal cancer, thyroid cancer, and non-small cell lung cancer. Following this, downstream mature bodies mir-19-3p and mir-19-5p were obtained by miRNA-lncRNA interaction analysis. Downstream mir-19-3p can functionally inhibit protein translation of CCNA2 in the human body, thus affecting learning ability and memory in the brain [13].

NBR2, as a non-coding RNA, is not involved in protein translation, so we intersected its related gene data with data on highly expressed proteins in brain tissues and finally selected GJA1 as a subsequent target gene. GJA1, also known as connexin 43 (Cx43), functions as a connexin hemichannel and is involved in paracrine processes [22]. GJAI is predominantly expressed in mature astrocytes, and astrocyte gap junctions are critical for neuronal function. GJA1 was demonstrated to affect AD development by altering astrocyte function in a study by Yuji Kajiwara et al. This is consistent with our findings.

Disease development is often not limited to single-gene defects, and our study explores the role of related gene clusters in AD development centered on target genes and more comprehensively demonstrates the function of NBR2 in this context. Based on the coordinated interactions of the gene clusters, we used a drug-disease proximity measure to establish a gene-drug interaction network for predicting potential therapeutic drugs [23]. This method mainly uses the distance between the target gene corresponding to the drug and the target gene corresponding to the disease to indicate medicinal potential of medicines. The "proximal drugs" intervene in the endocrine system and metabolic processes, while the "distal drugs" are mainly anti-inflammatory and pain relieving. We primarily screened cephalosporin antibiotics and adapalene, currently used as antibacterial and anti-inflammatory drugs [21, 24]. Interestingly, the drug Rubidium Chloride Rb-82 was found, a radioactive substance currently used in PET CT for the diagnosis of coronary heart disease and myocardial infarction [25].

Our study also has some limitations. Firstly, there is a lack of molecular biology experiments as additional validation. Secondly, there is no validation in terms of LTL in patients who clinically develop AD. In conclusion, we verified the causal link between LTL and AD using Mendelian randomization analysis and associated LTL-related lncRNAs. The downstream target genes were obtained by screening through interactions network analysis, which was used as a basis to explore the potential therapeutic drugs that might correspond to the relevant gene clusters. The evidence that LTL is associated with AD at the SNP level was supplemented, and the new gene-drug interaction network was used to screen for possible therapeutic drugs, providing fresh ideas for slowing down AD progression.

AUTHOR CONTRIBUTIONS

MZ and QY conceived the project. WL, HC, XY, and MZ completed revisions of article. MZ and HC wrote the manuscript. MZ and WL performed the data analysis mentioned in the paper. All authors commented on previous versions of the manuscript. All authors read and approved the final manuscript.

CONFLICTS OF INTEREST

The authors declare that they have no conflicts of interest.

FUNDING

No funding was provided for this study.

REFERENCES

1. Cao M, Li H, Zhao J, Cui J, Hu G. Identification of age- and gender-associated long noncoding RNAs in the human brain with Alzheimer's disease. Neurobiol Aging. 2019; 81:116–26. https://doi.org/10.1016/j.neurobiolaging.2019.05.023 PMID:31280115

2. Yang D, Huang R, Yoo SH, Shin MJ, Yoon JA, Shin YI, Hong KS. Detection of Mild Cognitive Impairment Using Convolutional Neural Network: Temporal-Feature Maps of Functional Near-Infrared Spectroscopy. Front Aging Neurosci. 2020; 12:141. https://doi.org/10.3389/fnagi.2020.00141 PMID:32508627

3. Lynch-Sutherland CF, Chatterjee A, Stockwell PA, Eccles MR, Macaulay EC. Reawakening the Developmental Origins of Cancer Through Transposable Elements. Front Oncol. 2020; 10:468. https://doi.org/10.3389/fonc.2020.00468 PMID:32432029

4. Ferreira MS, Sørensen MD, Pusch S, Beier D, Bouillon AS, Kristensen BW, Brümmendorf TH, Beier CP, Beier F. Alternative lengthening of telomeres is the major telomere maintenance mechanism in astrocytoma with isocitrate dehydrogenase 1 mutation. J Neurooncol. 2020; 147:1–14. https://doi.org/10.1007/s11060-020-03394-y PMID:31960234

5. Azarm K, Bhardwaj A, Kim E, Smith S. Persistent telomere cohesion protects aged cells from premature senescence. Nat Commun. 2020; 11:3321. https://doi.org/10.1038/s41467-020-17133-4 PMID:32620872

6. Mazidi M, Kengne AP, Vatanparast H. Food Security and Leukocyte Telomere Length in Adult Americans. Oxid Med Cell Longev. 2017; 2017:5427657. https://doi.org/10.1155/2017/5427657 PMID:28951768

7. Salmena L, Poliseno L, Tay Y, Kats L, Pandolfi PP. A ceRNA hypothesis: the Rosetta Stone of a hidden RNA language? Cell. 2011; 146:353–58. https://doi.org/10.1016/j.cell.2011.07.014 PMID:21802130

8. Su L, Li R, Zhang Z, Liu J, Du J, Wei H. Identification of altered exosomal microRNAs and mRNAs in Alzheimer's disease. Ageing Res Rev. 2022; 73:101497. https://doi.org/10.1016/j.arr.2021.101497 PMID:34710587

9. Zhang P, Sun J, Liang C, Gu B, Xu Y, Lu H, Cao B, Xu H. lncRNA IGHC γ 1 Acts as a ceRNA to Regulate Macrophage Inflammation via the miR-6891-3p/TLR4 Axis in Osteoarthritis. Mediators Inflamm. 2020; 2020:9743037. https://doi.org/10.1155/2020/9743037 PMID:32410875

10. Yin X, Xin H, Mao S, Wu G, Guo L. The Role of Autophagy in Sepsis: Protection and Injury to Organs. Front Physiol. 2019; 10:1071. https://doi.org/10.3389/fphys.2019.01071 PMID:31507440

11. Jin J, Kim SN, Liu X, Zhang H, Zhang C, Seo JS, Kim Y, Sun T. miR-17-92 Cluster Regulates Adult Hippocampal Neurogenesis, Anxiety, and Depression. Cell Rep. 2016; 16:1653–63. https://doi.org/10.1016/j.celrep.2016.06.101 PMID:27477270

12. Moustafa AA, Kim H, Albeltagy RS, El-Habit OH, Abdel-Mageed AB. MicroRNAs in prostate cancer: From function to biomarker discovery. Exp Biol Med (Maywood). 2018; 243:817–25. https://doi.org/10.1177/1535370218775657 PMID:29932371

13. Zhao X, Jin Y, Li H, Jia Y, Wang Y. Sevoflurane impairs learning and memory of the developing brain through post-transcriptional inhibition of CCNA2 via microRNA-19-3p. Aging (Albany NY). 2018; 10:3794–805. https://doi.org/10.18632/aging.101673 PMID:30540563

14. Zhu Z, Zhang F, Hu H, Bakshi A, Robinson MR, Powell JE, Montgomery GW, Goddard ME, Wray NR, Visscher PM, Yang J. Integration of summary data from GWAS and eQTL studies predicts complex trait gene targets. Nat Genet. 2016; 48:481–87. https://doi.org/10.1038/ng.3538 PMID:27019110

15. Bountziouka V, Nelson CP, Codd V, Wang Q, Musicha C, Allara E, Kaptoge S, Di Angelantonio E, Butterworth AS, Thompson JR, Curtis EM, Wood AM, Danesh JN, et al. Association of shorter leucocyte telomere length with risk of frailty. J Cachexia Sarcopenia Muscle. 2022; 13:1741–51. https://doi.org/10.1002/jcsm.12971 PMID:35297226

16. Scarabino D, Broggio E, Gambina G, Corbo RM. Leukocyte telomere length in mild cognitive impairment and Alzheimer's disease patients. Exp Gerontol. 2017; 98:143–7. https://doi.org/10.1016/j.exger.2017.08.025 PMID:28827085

17. Ramírez-Sanabria M, Martínez-Magaña J, Nicolini-Sánchez H, Guzmán-Sánchez R, Genis-Mendoza AD. Asociación entre la longitud de los telómeros y deterioro cognitivo en adultos mayores [Association between telomere length and cognitive impairment in older adults]. Rev Esp Geriatr Gerontol. 2022; 57:320–4. https://doi.org/10.1016/j.regg.2022.09.006 PMID:36319501

18. Ashrafi A, Cosentino S, Kang MS, Lee JH, Schupf N, Andersen SL, Christensen K, Province MA, Thyagarajan B, Zmuda JM, Honig LS. Leukocyte Telomere Length Is Unrelated to Cognitive Performance Among Non-Demented and Demented Persons: An Examination of Long Life Family Study Participants. J Int Neuropsychol Soc. 2020; 26:906–17. https://doi.org/10.1017/S1355617720000363 PMID:32342830

19. Warner KD, Hajdin CE, Weeks KM. Principles for targeting RNA with drug-like small molecules. Nat Rev Drug Discov. 2018; 17:547–58. https://doi.org/10.1038/nrd.2018.93 PMID:29977051

20. Ma N, Tie C, Yu B, Zhang W, Wan J. Identifying lncRNA-miRNA-mRNA networks to investigate Alzheimer's disease pathogenesis and therapy strategy. Aging (Albany NY). 2020; 12:2897–920.

https://doi.org/10.18632/aging.102785
PMID:32035423

21. Liu X, Xiao ZD, Han L, Zhang J, Lee SW, Wang W, Lee H, Zhuang L, Chen J, Lin HK, Wang J, Liang H, Gan B. LncRNA NBR2 engages a metabolic checkpoint by regulating AMPK under energy stress. Nat Cell Biol. 2016; 18:431–42.
https://doi.org/10.1038/ncb3328
PMID:26999735

22. Kajiwara Y, Wang E, Wang M, Sin WC, Brennand KJ, Schadt E, Naus CC, Buxbaum J, Zhang B. GJA1 (connexin43) is a key regulator of Alzheimer's disease pathogenesis. Acta Neuropathol Commun. 2018; 6:144.
https://doi.org/10.1186/s40478-018-0642-x
PMID:30577786

23. Guney E, Menche J, Vidal M, Barábasi AL. Network-based *in silico* drug efficacy screening. Nat Commun. 2016; 7:10331.
https://doi.org/10.1038/ncomms10331
PMID:26831545

24. Tolaymat L, Dearborn H, Zito PM. Adapalene. 2023 Jun 26. In: StatPearls [Internet]. Treasure Island (FL): StatPearls Publishing. 2024.
PMID:29494115

25. Rubidium Chloride Rb 82. Drugs and Lactation Database (LactMed(R)). Bethesda (MD). 2006.

SUPPLEMENTARY MATERIALS

Supplementary Tables

Please browse Full Text version to see the data of Supplementary Tables 4–7, 9, 10.

Supplementary Table 1. IVs associated with LTL on AD.

IVs associated with LTL on AD			
SNP	**beta**	**se**	**p**
rs10112752	0.036245368586056	0.335960595885184	0.914086302744282
rs1023767	0.0318330876610498	0.598202328717915	0.957560936273678
rs10845387	-2.23439804521506	0.770868499879615	0.00374896940811539
rs111527438	0.1226420207984	0.808320154808	0.879404184404874
rs115610405	0.135653125047028	0.331921070657474	0.682766504041688
rs11579626	-0.67653853842701	0.635972285930905	0.287425566351911
rs11646283	-1.03276164498491	0.633135927317576	0.102851350253984
rs11866592	-0.0888565421036374	0.395789941163395	0.82236492450604
rs12369950	-0.725930392584741	0.777176784832986	0.350272515749782
rs12613375	0.299590252043144	0.760846716847368	0.693758967833938
rs1291143	0.432281913149277	0.275809968471748	0.117040392785504
rs12941945	-0.631233574145798	0.497076375695793	0.204122915970736
rs13129697	-0.228596347825633	0.621621569699291	0.713065633921282
rs13230646	-0.839831534225546	0.628136900332993	0.181216141950711
rs1332941	-0.291483776011881	0.509999966268047	0.56763578614708
rs137901416	-0.353778125262467	0.340121648626422	0.298269407866343
rs139795227	-0.00912506310327856	0.734918273251148	0.990093374787841
rs144204502	-0.438618984202677	0.433917038694891	0.312094907111989
rs181647350	-0.914382859633444	0.345861126355731	0.00819844323220483
rs182059586	-0.211057336184845	0.657071988141656	'0.748052127615715
rs1907702	-0.519608790891665	0.769743554453666	0.49964944245128
rs1980240	0.105908226509547	0.745852568573192	0.887083011457418
rs1985369	0.669705295816193	0.465126151917485	0.149913853461556
rs2056726	0.147247860566561	0.498332026017415	0.767626134727134
rs2293607	-0.175791281699995	0.117004673984947	0.132986205123189
rs2303262	0.144742056923011	0.239692079898186	0.545932293003809
rs28502153	-0.0549658376581634	0.45240063767391	0.903296484974332
rs3093888	0.144358322298347	0.737626939057053	0.844839964712432
rs35640778	-0.589704286884422	0.170306915828354	0.000534988207818243
rs35671754	0.714915646701244	0.829696721453537	0.388875194050772
rs3891167	-0.290018592562576	0.278978713760175	0.298538569329448
rs4435700	-0.308159027472066	0.211939422991374'	0.145947475094368
rs4498805	0.741224448277236	0.629774507033154	0.23920827482734
rs4530278	-0.11801644199059	0.70674935941438	0.867381962574147
rs4724	0.0975753234171041	0.279984255974105	0.727462540965029
rs4743037	-1.23284685697873	0.762271434828446	0.105806388376798
rs4758644	-1.18132171212357	0.643015661549952	0.0661864946541454
rs61748181	-0.500385615307278	0.521266249933256	0.3370841662439
rs6590343	-1.51702332287106	0.795494585870592	0.056518121731675
rs6669563	-0.44839645574255	0.524620452345387	0.39271370915957
rs66731853	-1.21970213478748	0.567512463437407	0.031617942178875

rs6776756	-0.53846106593193	0.555723139539896	0.332576305186575
rs73581419	0.247682240388448	0.662445036765026	0.708485409074085
rs76219171	-0.413438596483427	0.564119745961388	0.463624575693405
rs762810	-0.108553589522824	0.491309870506245	0.825133467053132
rs76666449	0.268208322473189	0.528839065080898	0.612039504295859
rs7705526	-0.445782206505743	0.142292531483644	0.00173113540311976
rs7790856	-0.0192834938678268	0.238335937959602	0.935514417689642
rs78491606	-0.421827731636853	0.561317277459934	0.452354161193265
rs79228077	-0.554057619040488	0.76235760281677	0.467367680235681
rs80324517	0.151612587526323	0.559452787897053	0.786389819706275
rs8102497	1.09352745001804	0.641690413812528	0.0883557653618294
rs8105767	0.237753801447695	0.319336341283376	0.456559089212273
rs869785	1.87629640573512	0.677902038118029	0.00564362956915102
rs871134	1.16439596808499	0.530562251542741	0.0281890491407611
rs932002	0.0533718458002945	0.324472234345309	0.869346854618042
rs939916	0.13349415552803	0.424216473992432	0.75300156033797
rs9419958	-0.318804296586339	0.170001746112199	0.0607514454952407
rs9923119	1.66453409680992	0.674964337571699	0.0136590626994769

Supplementary Table 2. Mendelian randomization of exposures on the risk for AD.

Mendelian randomization of exposures on the risk for AD							
Method	**nsnp**	**beta**	**se**	**pval**	**OR**	**or_lci95**	**or_uci95**
MR Egger	59	-0.284772361	0.096200533	0.004473661	0.7521855	0.6229273	0.9082648
Weighted median	59	-0.204963971	0.07786336	0.008479532	0.8146767	0.6993694	0.948995
Inverse variance weighted	59	-0.192330809	0.057355096	0.000798442	0.8250339	0.73731	0.923195
Simple mode	59	0.022117346	0.159358624	0.890097059	1.0223637	0.7480948	1.397186
Weighted mode	59	-0.266739507	0.083141208	0.002175884	0.7658725	0.6507067	0.9014211

Supplementary Table 3. Pleiotropy and heterogeneity of the causal association between LTL and AD.

Heterogeneity			
Method	**Q**	**Q_df**	**Q-p-val**
MR Egger	86.80831	57	0.006663209
Inverse variance weighted	88.98135	58	0.005524221
Pleiotropy			
Method			**p-val**
egger_intercept			0.237224

Supplementary Table 4. SMR analysis for cis-eQTL genetic variants used as the IVs for gene expression.

Supplementary Table 5. The mRNA targets of miR-19-3p predicted.

Supplementary Table 6. The mRNA targets of miR-19-5p predicted.

Supplementary Table 7. The gene names of upregulated expressed proteins in Alzheimer's disease (AD) brain drawn from public data (https://doi.org/10.1038/s41593-021-00999-y).

Supplementary Table 8. The list of genes associated with GJA1 in AD brain tissue.

gene_name1	gene_name2	cor_r	p-value
GJA1	ADD3	0.802371206904213	1.17341269039321E-21
GJA1	CSRP1	0.820254711108708	2.61773616426948E-23
GJA1	SLC39A12	0.801549080433322	1.38449947933484E-21
GJA1	GABRG3	-0.637275526922121	1.1080578580304E-11
GJA1	GFRA2	-0.607471408	1.71921683018262E-10
GJA1	GJA1	1	0
GJA1	GOT1	-0.608856007508237	1.52315537236684E-10
GJA1	ICA1	-0.602400596892852	2.66545497842034E-10
GJA1	IDH3G	-0.626270516361077	3.15525095511253E-11
GJA1	ATP1A2	0.824295131116415	1.04551338281366E-23
GJA1	NOTCH2	0.808104375749031	3.62158286681252E-22
GJA1	PAX6	0.822685726261586	1.51115845882501E-23
GJA1	GRAMD1C	0.816757790187561	5.68767509823794E-23
GJA1	PLSCR4	0.83129683399707	2.0132995105433E-24
GJA1	RASGRF1	-0.601698028693054	2.83070247178229E-10
GJA1	GRAMD3	0.829356830850272	3.20169444474726E-24
GJA1	BEND5	-0.614344090684302	9.37105215524573E-11
GJA1	CC01	-0.615299465425736	8.60296422575356E-11
GJA1	HSPB3	-0.636926806041838	1.14615294142954E-11

Supplementary Table 9. Gene Ontology (GO) enrichment analysis results.

Supplementary Table 10. Kyoto Encyclopedia of Genes and Genomes (KEGG) enrichment pathway annotated classification results.